Military Technical College
Kobry El-Kobbah,
Cairo, Egypt.

13th International Conference on Applied Mechanics and Mechanical Engineering.

THE EFFECTS OF CENTRIPETAL AND CORIOLIS FORCES ON THE DYNAMIC RESPONSE OF A CRACKED BEAM UNDER A MOVING MASS LOAD

REİS* M. and PALA ** Y.

ABSTRACT

This study is devoted to the investigation of the effects of centripetal and Coriolis forces on the forced vibration of a simply supported beam with a single crack under moving mass load. As in the case of beams without a crack, it is shown that these forces must be considered in the analysis. The combined effects of these forces are especially important for the cracked long beams. The response of the system is obtained in terms of Duhamel integral. The differential equation which involves a non-linearity on its right hand side is solved via an iterative procedure. The results are exemplified for various values of the variables.

KEYWORDS

Beams, centripetal, Coriolis, crack, moving mass.

NOMENCLATURE

E	Modulus of elasticity (N/m^2)
I	Second moment of area for the cross-section of the beam (m^4)
Y,y	Vertical deflection of the beam (m), dimensionless vertical deflection of the beam
X,x	Horizontal location of the beam (m), dimensionless horizontal location of the beam
T,t	Time (sec), modified time
L,l	Length of the beam (m), dimensionless length of the beam
L_0,l_0	Position of the crack (m), dimensionless position of the crack
V,v	Velocity of the moving mass (m/sec), modified velocity of the moving mass
g	Gravity (m/sec^2)
ρA	Density of the beam (kg/m^3), Cross-section of the beam (m^2)
B,H,D	Width of the beam (m), Height of the beam (m), Depth of the crack (m)
γ	Non-dimensional crack-depth ratio
θ	Non-dimensional crack sectional flexibility
λ	Eigen-values of free vibration

* Graduate student, Dpt. of Mechanical Engineering, Uludağ University, Bursa, Turkey
** Professor, Dpt. of Mechanical Engineering, Uludağ University, Bursa, Turkey.

INTRODUCTION

The dynamic response of beams under moving forces or masses has been investigated for more than a century. A wealthy of results, both analytical and experimental, were tabulated for a number of cases, different in loading and geometry. The reason for these studies is the observations that as a beam structure is subjected to moving loads, the dynamic transversal deflection as well as the stresses could become significantly higher than those for the static load could. After substantial works have been carried out in this field, researchers have tent to studying the dynamics of cracked structures in the last decade. Indeed, the existence of crack induces a local flexibility which is a function of the crack depth, thereby changing its dynamic behavior and its stability characteristic [1]. The dynamic behavior of cracked structures has been investigated by many analytical and computational methods [2,3,4,5,6]. While some of these researchers were dealt with the detection of crack, some others were based on investigating the effects of cracks on the frequencies of the beam. Dimarogonas gave a review of the dynamics of cracked structures [3]. The continuous cracked beam vibration theory was developed by Chondros et al. for the lateral vibration of cracked Euler-Bernoulli beams with single-edge or double-edge open cracks [7]. Ostachowitz and Krawezuk presented a method analysis of the effect of two open crack upon the frequencies of the natural flexural vibrations in a cantilever beam [8]. Rizos and Aspragathos used a rotational spring to model the crack and detect the crack location through the measurement of the amplitudes of the component [9]. Liang et al. studied a similar problem by finite element method [10]. Lin et al. have studied beam vibrations with an arbitrary number of cracks using a hybrid analytical/numerical method that permits the efficient computations of the eigen-solutions for various boundary conditions [11]. Each crack was presented by a massless rotational spring with sectional flexibility in this work. Transfer matrix method has been efficiently used to reduce the number of constants of the eigen-functions which are solved through the satisfaction of boundary conditions.

As for the dynamics response of cracked beams under moving forces or loads, not much work is available in the literature. Parhi and Behera [12] used the Runge-Kutta method to find the deflection of a cracked circular shaft subjected to a moving load. Mahmoud used an equivalent static load approach to determine the stress intensity factors for a cracked beam under moving load [13]. Mahmoud and Zaid [14] used an iterative modal analysis approach to determine the cracked beam's response. Most of these works have analyzed the problem numerically or hybrid numerically. Lin et al. presented an extended method for the beam vibrations with an arbitrary number of cracks for obtaining the modes and frequencies of the system [6]. Lin et al. analyzed the forced response of a cracked cantilever beam under a concentrated moving load [15]. In this paper, the cracked beam system was modeled as a two-span beam, each of which obeys Euler-Bernoulli beam theory. Forced response was obtained by the modal expansion theory using the determined eigen-functions. However, as is proved in the following paragraphs, the method presented is deficient in many respects and must be reformulated.

In analyzing the response of cracked beams under moving loads, centripetal and Coriolis forces were always neglected. However, as was proved by Michaltsos and Kounadis [16] for the case of un-cracked beams, these terms can appreciably affect the beam response and must be inserted into the theory depending upon the beam's size and the velocity of the moving mass.

Therefore, the present work inserts the effects of centripetal and Coriolis forces into the dynamic analysis of simply supported beams with a crack under moving mass load. It should be expected that the existence of mass rather than a force and a crack in the analysis makes the formulation much complicated. The reason for this complexity is the existence of nonlinear terms on the right hand side of the differential equation in the case of mass loads. The analysis is performed for a single-side crack. Forced response is obtained in terms of Duhamel integrals.

Eigen-Value Analysis

Let us consider a hinged-hinged beam of length *L* with an open crack located at $x = L_0$. A body of mass *M* is moving on the beam with a constant velocity *V*. The dimensions of the uniform cross-section of the beam are: width *B*, height *H* crack depth *D* (Fig. 1). The crack divides the beam into two parts. According to Euler-Bernoulli beam theory, the equation of motion for each part in the case of free vibration can be written as

$$EI\frac{\partial^4 Y_1}{\partial X^4}+\rho A\frac{\partial^2 Y_1}{\partial T^2}=0, \qquad 0<X<L_0 \tag{1}$$

$$EI\frac{\partial^4 Y_2}{\partial X^4}+\rho A\frac{\partial^2 Y_2}{\partial T^2}=0, \qquad L_0<X<L \tag{2}$$

Here, Y_1 and Y_2 are the vertical displacements, ρA is the mass per unit length. The boundary conditions for a simply supported beam are given by

$$Y_1(0,T)=0, \quad Y_2(L,T)=0, \quad Y_1''(0,T)=0, \quad Y_2''(L,T)=0, \tag{3}$$

The compatibility requirements enforce continuities of the displacement, bending moment and shear force, respectively, across the crack and can be expressed as

$$Y_1(L_0^-,T)=Y_2(L_0^+,T), \tag{4}$$

$$Y_1''(L_0^-,T)=Y_2''(L_0^+,T), \tag{5}$$

$$Y_1'''(L_0^-,T)=Y_2'''(L_0^+,T), \tag{6}$$

Here, L_0^+, L_0^- denote the locations immediately above and below the crack position, respectively. Discontinuity condition at the crack can be written as

$$Y_2'(L_0^+,T)-Y_1'(L_0^-,T)=\theta_1 L Y_2''(L_0^+,T), \tag{7}$$

where θ_1 is the non-dimensional crack sectional flexibility, which is a function of the crack extent [4]. For a single sided open crack [8],

$$\theta_1=6\pi\gamma^2 f(\gamma)\left(\frac{H}{L}\right) \tag{8}$$

Here, $\gamma=D/H$ is the non-dimensional crack-depth ratio, and

$$f(\gamma) = 0.6384 - 1.035\gamma + 3.7201\gamma^2 - 5.177\gamma^3 + 7.553\gamma^4 - 7.332\gamma^5 + 2.4909\gamma^6 \tag{9}$$

and, for a double sided crack [8]

$$\theta_1 = 6\pi\gamma^2 f(\gamma)\left(\frac{H}{L}\right) \tag{10}$$

$$f(\gamma) = 0.5335 - 0.929\gamma + 3.5\gamma^2 - 3.181\gamma^3 + 5.793\gamma^4 \tag{11}$$

We introduce the following parameters:

$$y_1 = \frac{Y_1}{L},\ y_2 = \frac{Y_2}{L},\ l_1 = \frac{L_1}{L},\ l_2 = \frac{L_2}{L},\ x = \frac{X}{L} \tag{12}$$

$$x_1 = \frac{X_1}{L},\ x_2 = \frac{X_2}{L},\ v = \frac{V}{\sqrt{L}},\ t = \frac{T}{\sqrt{L}}, \tag{13}$$

Thus, Eqs. (1) and (2) can be written as

$$\frac{EI}{L^3}\frac{\partial^4 y_1}{\partial x^4} + \rho A\frac{\partial^2 y_1}{\partial t^2} = 0, \qquad 0 < x < \frac{L_0}{L} \tag{14}$$

$$\frac{EI}{L^3}\frac{\partial^4 y_2}{\partial x^4} + \rho A\frac{\partial^2 y_2}{\partial t^2} = 0, \qquad \frac{L_0}{L} < x < 1 \tag{15}$$

The conditions imposed on the problem then become

$$y_1(0,t) = 0,\quad y_2(1,t) = 0,\quad y_1''(0,t) = 0,\quad y_2''(1,t) = 0$$

$$y_1\left(\frac{L_0^-}{L},t\right) = y_2\left(\frac{L_0^+}{L},t\right),\qquad y_1''\left(\frac{L_0^-}{L},t\right) = y_2''\left(\frac{L_0^+}{L},t\right),\qquad y_1'''\left(\frac{L_0^-}{L},t\right) = y_2'''\left(\frac{L_0^+}{L},t\right), \tag{16}$$

$$y_2'\left(\frac{L_0^+}{L},t\right) - y_1'\left(\frac{L_0^-}{L},t\right) = \theta_1 y_2''\left(\frac{L_0^+}{L},t\right) \tag{17}$$

Using the separable solution $y_{(i)}(x,t) = \phi_i(x)e^{i\omega t}$, $i = 1,2$ in Eqs.(14) and (15) lead to

$$\phi_1^{IV}(x) - \lambda^4\phi_1(x) = 0, \qquad 0 < x < \frac{L_0}{L} \tag{18}$$

$$\phi_2^{IV}(x) - \lambda^4\phi_2(x) = 0, \qquad \frac{L_0}{L} < x < 1 \tag{19}$$

where

$$\lambda^4 = \frac{\rho A\omega^2 L^3}{EI} \tag{20}$$

Using Eqs.(16) and (17) , the conditions on ϕ_1 and ϕ_2 are readily obtained as:

$$\phi_1\left(\frac{L_0^-}{L}\right)=\phi_2\left(\frac{L_0^+}{L}\right),\quad \phi_1''\left(\frac{L_0^-}{L}\right)=\phi_2''\left(\frac{L_0^+}{L}\right),\quad \phi_1'''\left(\frac{L_0^-}{L}\right)=\phi_2'''\left(\frac{L_0^+}{L}\right) \tag{21}$$

$$\phi_2'\left(\frac{L_0^-}{L}\right)-\phi_1'\left(\frac{L_0^+}{L}\right)=\theta_1\phi_2''\left(\frac{L_0^+}{L}\right) \tag{22}$$

On the other hand, using the boundary conditions in Eqs.(16) , we obtain

$$\phi_1(0)=0,\qquad \phi_2(1)=0,\qquad \phi_1''(0)=0,\qquad \phi_1''(1)=0 \tag{23}$$

The solutions of Eq.(18) and Eq.(19) can be shown to be

$$\phi_1(x)=A_1\sin\lambda(x)+B_1\cos\lambda(x)+C_1\sinh\lambda(x)+D_1\cosh\lambda(x),\qquad 0<x<\frac{L_0}{L} \tag{24}$$

$$\phi_2(x)=A_2\sin\lambda\left(x-\frac{L_0}{L}\right)+B_2\cos\lambda\left(x-\frac{L_0}{L}\right)+C_2\sinh\lambda\left(x-\frac{L_0}{L}\right)+D_2\cosh\lambda\left(x-\frac{L_0}{L}\right),\qquad \frac{L_0}{L}<x<1 \tag{25}$$

where A's , B's , C's and D's are constants to be determined . Using the conditions given by Eq.(23)

$$B_1=D_1=0 \tag{26}$$

Second and fourth conditions on $\phi_2(x)$ yield

$$0=A_2\sin\lambda\left(\frac{L-L_0}{L}\right)+B_2\cos\lambda\left(\frac{L-L_0}{L}\right)+C_2\sinh\lambda\left(\frac{L-L_0}{L}\right)+D_2\cosh\lambda\left(\frac{L-L_0}{L}\right) \tag{27}$$

$$0=-A_2\sin\lambda\left(\frac{L-L_0}{L}\right)-B_2\cos\lambda\left(\frac{L-L_0}{L}\right)+C_2\sinh\lambda\left(\frac{L-L_0}{L}\right)+D_2\cosh\lambda\left(\frac{L-L_0}{L}\right) \tag{28}$$

Eqs.(27) and (28) can be written in matrix form as

$$\begin{bmatrix}0\\0\end{bmatrix}=\begin{bmatrix}\sin\lambda\left(\frac{L-L_0}{L}\right) & \cos\lambda\left(\frac{L-L_0}{L}\right) & \sinh\lambda\left(\frac{L-L_0}{L}\right) & \cosh\lambda\left(\frac{L-L_0}{L}\right)\\ -\sin\lambda\left(\frac{L-L_0}{L}\right) & -\cos\lambda\left(\frac{L-L_0}{L}\right) & \sinh\lambda\left(\frac{L-L_0}{L}\right) & \cosh\lambda\left(\frac{L-L_0}{L}\right)\end{bmatrix}\begin{bmatrix}A_2\\B_2\\C_2\\D_2\end{bmatrix} \tag{29}$$

or

$$\begin{bmatrix}0\\0\end{bmatrix}=B_{2\times4}\begin{bmatrix}A_2\\B_2\\C_2\\D_2\end{bmatrix} \tag{30}$$

Using the matching conditions at the crack where $x = L_0$, we have

$$\phi_1'''\left(\frac{L_0^-}{L}\right) = \phi_2'''\left(\frac{L_0^+}{L}\right):$$

$$-A_2 + C_2 = -A_1 c\,\mathrm{os}\,\lambda\left(\frac{L_0}{L}\right) + B_1 \sin\lambda\left(\frac{L_0}{L}\right) + C_1 \cosh\lambda\left(\frac{L_0}{L}\right) + D_1 \sinh\lambda\left(\frac{L_0}{L}\right) \quad (31)$$

$$\phi_2' - \phi_1' = \theta_1 \phi_2''\left(\frac{L_0}{L}\right):$$

$$A_2 + C_2 - A_1 c\,\mathrm{os}\,\lambda\left(\frac{L_0}{L}\right) + \mathrm{B}_1 \sin\lambda\left(\frac{L_0}{L}\right) - C_1 \cosh\lambda\left(\frac{L_0}{L}\right) - D_1 \sinh\lambda\left(\frac{L_0}{L}\right) + \theta_1 B_2\lambda - \theta_1 D_2\lambda = 0 \quad (32)$$

$$\phi_1\left(\frac{L_0}{L}\right) = \phi_2\left(\frac{L_0}{L}\right):$$

$$B_2 + D_2 = A_1 \sin\lambda\left(\frac{L_0}{L}\right) + B_1 co\,\mathrm{s}\,\lambda\left(\frac{L_0}{L}\right) + C_1 \sinh\lambda\left(\frac{L_0}{L}\right) + D_1 co\,\mathrm{sh}\,\lambda\left(\frac{L_0}{L}\right) \quad (33)$$

$$\phi_1''\left(\frac{L_0}{L}\right) = \phi_2''\left(\frac{L_0}{L}\right):$$

$$B_2 - D_2 = A_1 \sin\lambda\left(\frac{L_0}{L}\right) + B_1 co\,\mathrm{s}\,\lambda\left(\frac{L_0}{L}\right) - C_1 \sinh\lambda\left(\frac{L_0}{L}\right) - D_1 co\,\mathrm{sh}\,\lambda\left(\frac{L_0}{L}\right) \quad (34)$$

Eqs.(31),(32),(33) and (34) can be written in matrix form as

$$\begin{bmatrix} A_2 \\ B_2 \\ C_2 \\ D_2 \end{bmatrix} = \begin{bmatrix} t_{11} & t_{12} & t_{13} & t_{14} \\ t_{21} & t_{22} & t_{23} & t_{24} \\ t_{31} & t_{32} & t_{33} & t_{34} \\ t_{41} & t_{42} & t_{43} & t_{44} \end{bmatrix} \begin{bmatrix} A_1 \\ B_1 \\ C_1 \\ D_1 \end{bmatrix} \quad (35)$$

or

$$\begin{bmatrix} A_2 \\ B_2 \\ C_2 \\ D_2 \end{bmatrix} = T_{4\times4} \begin{bmatrix} A_1 \\ B_1 \\ C_1 \\ D_1 \end{bmatrix} \quad (36)$$

where

$$t_{11}=\cos\lambda\left(\frac{L_0}{L}\right)-\frac{\theta_1\lambda}{2}\sin\lambda\left(\frac{L_0}{L}\right),\qquad t_{12}=-\sin\lambda\left(\frac{L_0}{L}\right)-\frac{\theta_1\lambda}{2}\cos\lambda\left(\frac{L_0}{L}\right),$$

$$t_{13}=-\frac{\theta_1\lambda}{2}\sin\lambda\left(\frac{L_0}{L}\right),\qquad t_{14}=\frac{\theta_1\lambda}{2}\cosh\lambda\left(\frac{L_0}{L}\right),$$

$$t_{21}=\sin\lambda\left(\frac{L_0}{L}\right),\quad t_{22}=\cos\lambda\left(\frac{L_0}{L}\right),\quad t_{23}=0,\quad t_{24}=0,$$

$$t_{31}=-\frac{\theta_1\lambda}{2}\sin\lambda\left(\frac{L_0}{L}\right),\qquad t_{32}=-\frac{\theta_1\lambda}{2}\cos\lambda\left(\frac{L_0}{L}\right),$$

$$t_{33}=\cosh\lambda\left(\frac{L_0}{L}\right)+\frac{\theta_1\lambda}{2}\sin h\lambda\left(\frac{L_0}{L}\right),\qquad t_{34}=\sinh\lambda\left(\frac{L_0}{L}\right)+\frac{\theta_1\lambda}{2}\cos h\lambda\left(\frac{L_0}{L}\right),$$

$$t_{41}=0,\quad t_{42}=0,\quad t_{43}=\sinh\lambda\left(\frac{L_0}{L}\right),\quad t_{44}=\cosh\lambda\left(\frac{L_0}{L}\right) \tag{37}$$

Inserting Eq.(36) into Eq.(30) yields

$$\begin{bmatrix}0\\0\end{bmatrix}=B_{2\times4}\times T_{4\times4}\begin{bmatrix}A_1\\B_1\\C_1\\D_1\end{bmatrix}=R_{2\times4}\begin{bmatrix}A_1\\B_1\\C_1\\D_1\end{bmatrix}=R_{2\times4}\begin{bmatrix}A_1\\0\\C_1\\0\end{bmatrix} \tag{38}$$

where

$$R_{2\times4}=\begin{bmatrix}r_{11}&r_{12}&r_{13}&r_{14}\\r_{21}&r_{22}&r_{23}&r_{24}\end{bmatrix} \tag{39}$$

Here, the elements of $R_{2\times4}$ are given by

$$\begin{aligned}
r_{11}&=b_{11}t_{11}+b_{12}t_{21}+b_{13}t_{31}+b_{14}t_{41}\\
r_{12}&=b_{11}t_{12}+b_{12}t_{22}+b_{13}t_{32}+b_{24}t_{42}\\
r_{13}&=b_{11}t_{13}+b_{12}t_{23}+b_{13}t_{33}+b_{14}t_{43}\\
r_{14}&=b_{11}t_{14}+b_{12}t_{24}+b_{13}t_{34}+b_{14}t_{44}\\
r_{21}&=b_{21}t_{11}+b_{22}t_{21}+b_{23}t_{31}+b_{24}t_{41}\\
r_{22}&=b_{21}t_{12}+b_{22}t_{22}+b_{23}t_{32}+b_{24}t_{42}\\
r_{23}&=b_{21}t_{13}+b_{22}t_{23}+b_{23}t_{33}+b_{24}t_{43}\\
r_{24}&=b_{21}t_{14}+b_{22}t_{24}+b_{23}t_{34}+b_{24}t_{44}
\end{aligned} \tag{40}$$

The existence of non-trivial solutions requires

$$\det\begin{bmatrix}r_{11}&r_{13}\\r_{21}&r_{23}\end{bmatrix}=0 \tag{41}$$

Using Eqs.(26), (27), (28), (31), (32), (33) and (34), the following relations among *A*'s, *B*'s , *C*'s and *D*'s can be found :

$$\begin{aligned} &n_1 = \sin\lambda L_0, \quad n_2 = \cos\lambda L_0, \quad n_3 = \sinh\lambda L_0, \quad n_4 = \cosh\lambda L_0, \\ &n_5 = \sin\lambda(1-L_0), \quad n_6 = \cos\lambda(1-L_0), \quad n_7 = \sinh\lambda(1-L_0), \quad n_8 = \cosh\lambda(1-L_0) \end{aligned} \tag{42a}$$

$$\begin{aligned} &\mathrm{A}_2 = -O_1 A_1, \quad B_2 = n_1 A_1, \quad C_2 = -O_2 C_1, \quad D_2 = n_3 C_1, \\ &C_1 = \frac{n_1 + O_1}{n_4 + O_2} A_1, \quad \mathrm{O}_1 = \frac{n_1 n_6}{n_5}, \quad \mathrm{O}_2 = \frac{n_3 n_8}{n_7}, \quad C_1 = \frac{\frac{\theta_1 \lambda}{2} n_1}{\left[\frac{n_3 n_8}{n_7} + n_4\right]} \end{aligned} \tag{42b}$$

Eliminating all the coefficients in Eqs.(42a and 42b) , the frequency equation can also be obtained as

$$\left(\frac{\theta_1\lambda}{2}\right)^2 n_3 n_1 = \left(\frac{n_8 n_3}{n_7} + n_4 + \frac{\theta_1\lambda}{2} n_3\right)\left(\frac{n_6 n_1}{n_5} - \frac{\theta_1\lambda}{2} n_1 + n_2\right) \tag{43}$$

Eq.(43) derived in an abbreviated way is another form of the frequency equation given by Eq.(41), and yields the same values for λ's .

The equation of motion of the beam under a moving mass *M* can be written as [16]

$$EI\frac{\partial^4 Y_i}{\partial X^4} + \rho A\frac{\partial^2 Y_i}{\partial T^2} = M\left[g - a_M\right]\delta\left(X - VT\right), \qquad i = 1, 2, \ldots \tag{44}$$

Here, $\delta(X - VT)$ is Dirac's delta function. Since the transverse displacement *Y* is a function of *X* and time *T*, we obtain the transverse acceleration $\ddot{Y} = a_M$ as

$$a_M = \ddot{Y} + V^2 Y'' + 2V\dot{Y}' \tag{45}$$

where $\dot{Y}' = \partial^2 Y/\partial X \partial T$, $Y'' = \partial^2 Y/\partial X^2$, $\ddot{Y} = \partial^2 Y/\partial T^2$. The second and third terms on the right side of Eq.(45) correspond to the centrifugal and Coriolis accelerations. Inserting Eq.(45) into Eq.(44) yields

$$EI\frac{\partial^4 Y_i}{\partial X^4} + \rho A\frac{\partial^2 Y_i}{\partial T^2} = Mg\delta\left(X - VT\right) - M\left[\ddot{Y} + V^2 Y'' + 2V\dot{Y}'\right]\delta\left(X - VT\right) \tag{46}$$

We introduce the following quantities:

$$y_i = \frac{Y_i}{L}, \quad \mathrm{x} = \frac{X}{L}, \quad \ell_0 = \frac{L_0}{L}, \quad t = \frac{T_i}{\sqrt{L}}, \quad v = \frac{V}{\sqrt{L}} \tag{47}$$

Thus, in each segment, Eq.(46) can then be expressed in a non-dimensional form as

$$\frac{\partial^4 y_i}{\partial x^4} + \frac{\rho A L^3}{EI}\frac{\partial^2 y_i}{\partial t^2} = \frac{MgL^2}{EI}\delta\left(x - vt\right) - \frac{ML^2}{EI}\left[\ddot{y}_i + v^2 y_i'' + 2v\dot{y}_i'\right]\delta\left(x - vt\right) \tag{48}$$

A series solution of Eq.(48) can be sought in the form

$$y(x,t)=\sum_{n=0}^{N}\phi_n(x)q_n(t) \tag{49}$$

where normalized eigen-functions $\phi_n(x)$ of the cracked system are given by Eq.(24) and (25), $q_n(t)$ are the generalized coordinates and N is the number of eigen-functions used to approximate the solution.

Substituting Eq.(49) into Eq.(48), multiplying by $\phi_j(x)$ and integrating from 0 to 1 lead to

$$\begin{aligned}\sum_{n=1}^{N}\left[\frac{\rho AL^3}{EI}\ddot{q}_n+\lambda^4 q_n\right]\int_0^1\phi_m(x)\phi_n(x)dx=&\frac{MgL^2}{EI}\int_0^1\delta(x-vt)\phi_m(x)dx\\&-\frac{ML^2}{EI}\phi_n(vt)\left[\sum_{m=1}^{N}\ddot{q}_m\int_0^1\delta(x-vt)\phi_m(vt)\phi_m(x)dx\right]\\&-\frac{ML^2v^2}{EI}\phi_n''(vt)\left[\sum_{m=1}^{N}q_m\int_0^1\delta(x-vt)\phi_m(x)dx\right]\\&-\frac{2ML^2v}{EI}\phi_n'(vt)\left[\sum_{m=1}^{N}\dot{q}_m\int_0^1\delta(x-vt)\phi_m(x)dx\right]\end{aligned} \tag{50}$$

Using the ortogonality condition of eigen-functions, Eq.(50) can be written as

$$\begin{aligned}\ddot{q}_n+\omega_n^2q_n=Q_n(t)=&\frac{Mg}{\rho AL}\phi_n(vt)\\&-\frac{M}{\rho AL}\phi_n(vt)\left[\sum_{m=1}^{N}\ddot{q}_m\phi_m(vt)\right]-\frac{Mv^2}{\rho AL}\phi_n(vt)\left[\sum_{m=1}^{N}q_m\phi_m''(vt)\right]-\frac{2Mv}{\rho AL}\phi_n(vt)\left[\sum_{m=1}^{N}\dot{q}_m\phi_m'(vt)\right]\end{aligned} \tag{51}$$

A very important point that must be recalled here is that ,although the eigen-functions are orthogonal, they are not orthonormal in general. In other words, they result in $\int_0^1\phi_m{}^2dx=k$. In order to make this term normalized, the constant A's in the expressions for eigen-functions must be chosen as $A=1/\sqrt{k}$. However, this value must also take place on the right hand side of Eq.(51).

A closed form solution to Eq.(51) is not possible. However, we can seek approximate solution of Eq.(51). In order to solve Eq.(51), a technique developed by Michaltsos and Kounadis [16] will be used. This method has also been used by the writers in a different paper [17]. In fact, this method is a different version of Picard's method applied to non-linear ordinary differential equations in which the non-linearity takes place on the right side of the differential equation. According to this method, a first approximate solution of the differential equation is obtained by keeping only the first term on the right side of Eq.(51). This leads to

$$\ddot{q}_n + \omega_n^2 q_n = \frac{Mg}{\rho AL}\phi_n(vt) \tag{52}$$

or

$$\ddot{q}_n + \omega_n^2 q_n = \begin{cases} \dfrac{Mg}{\rho AL} f_{n1}(vt), & t \le \dfrac{L_0}{V\sqrt{L}} \\ \dfrac{Mg}{\rho AL} f_{n2}(vt), & t > \dfrac{L_0}{V\sqrt{L}} \end{cases} \tag{53}$$

where

$$f_{n1}(vt) = A_{n1}\sin\lambda(vt) + B_{n1}\cos\lambda(vt) + C_{n1}\sinh\lambda(vt) + D_{n1}\cosh\lambda(vt), \tag{54}$$

$$f_{n2}(vt) = A_{n2}\sin\lambda(vt) + B_{n2}\cos\lambda(vt) + C_{n2}\sinh\lambda(vt) + D_{n2}\cosh\lambda(vt), \tag{55}$$

The solution of the homogenous part of Eq.(51) for $t \le \dfrac{L_0}{V\sqrt{L}}$ is

$$(q_{n1})_h = d_1\sin\omega_n t + d_2\cos\omega_n t \tag{56}$$

where d_1, d_2 are constants to be determined. Let us assume that the proper solution to Eq.(51) has the form

$$(q_{n1})_p = \overline{A}_{n1}\sin\Omega_n t + \overline{B}_{n1}\cos\Omega_n t + \overline{C}_{n1}\sinh\Omega_n t + \overline{D}_{n1}\cosh\Omega_n t \tag{57}$$

where $\Omega_n = \lambda_n v$. Substituting Eq.(57) into Eq.(51) yields

$$\begin{aligned} \overline{A}_{n1} &= \frac{Mg}{\rho AL}\frac{A_{n1}}{\omega_n^2 - \Omega_n^2}, & \overline{B}_{n1} &= \frac{Mg}{\rho AL}\frac{B_{n1}}{\omega_n^2 - \Omega_n^2} \\ \overline{C}_{n1} &= \frac{Mg}{\rho AL}\frac{C_{n1}}{\omega_n^2 + \Omega_n^2}, & \overline{D}_{n1} &= \frac{Mg}{\rho AL}\frac{D_{n1}}{\omega_n^2 + \Omega_n^2} \end{aligned} \tag{58}$$

Thus, the general solution to Eq.(51) for $x < L_0 / L$ takes the form

$$q_{n1}(t) = d_1\sin\omega_n t + d_2\cos\omega_n t + (q_n)_p \tag{59}$$

In order to determine d_1 and d_2 in Eq.(59), we use the initial conditions $q_{n1}(0) = 0$ and $\dot{q}_{n1}(0) = 0$. After some operations, one readily finds

$$d_1 = -\frac{\Omega_n}{\omega_n}\left(\overline{A}_{n1} + \overline{C}_{n1}\right), \qquad d_2 = -\overline{B}_{n1} - \overline{D}_{n1} \tag{60}$$

The last form of $q_{n1}(t)$ in the first region can thus be written as

$$q_{n1}(t)\Big|_{t\le\frac{L_0}{V\sqrt{L}}} = -\frac{\Omega_n}{\omega_n}\left(\bar{A}_{n1}+\bar{C}_{n1}\right)\sin\omega_n t-\left(\bar{B}_{n1}+\bar{D}_{n1}\right)\cos\omega_n t + \bar{A}_{n1}\sin\Omega_n t+\bar{B}_{n1}\cos\Omega_n t+\bar{C}_{n1}\sinh\Omega_n t+\bar{D}_{n1}\cosh\Omega_n t \tag{61}$$

In the same manner, for $t>\dfrac{L_0}{V\sqrt{L}}$ the solution of homogeneous part and the proper solution can be written as

$$\left(q_{n2}\right)_h=\bar{d}_1\sin\omega_n t+\bar{d}_2\cos\omega_n t \tag{62}$$

and

$$\left(q_{n2}\right)_p=\bar{A}_{n2}\sin\Omega_n t+\bar{B}_{n2}\cos\Omega_n t+\bar{C}_{n2}\sinh\Omega_n t+\bar{D}_{n2}\cosh\Omega_n t \tag{63}$$

One can readily show that the coefficients in Eq.(63) are in the forms

$$\bar{A}_{n2}=\frac{Mg}{\rho AL}\frac{A_{n2}}{\omega_n^2-\Omega_n^2},\qquad \bar{B}_{n2}=\frac{Mg}{\rho AL}\frac{B_{n2}}{\omega_n^2-\Omega_n^2}$$
$$\bar{C}_{n2}=\frac{Mg}{\rho AL}\frac{C_{n2}}{\omega_n^2+\Omega_n^2},\qquad \bar{D}_{n2}=\frac{Mg}{\rho AL}\frac{D_{n2}}{\omega_n^2+\Omega_n^2} \tag{64}$$

Hence, the general solution of $q_{n2}(t)$ in the second region can be written as

$$q_{n2}(t)\Big|_{t>\frac{L_0}{V\sqrt{L}}} = (q_{n2})_h+(q_{n2})_p=\bar{d}_1\sin\omega_n t+\bar{d}_2\cos\omega_n t + \bar{A}_{n2}\sin\lambda\left(vt-\ell_0\right)+\bar{B}_{n2}\cos\lambda\left(vt-\ell_0\right)+\bar{C}_{n2}\sinh\lambda\left(vt-\ell_0\right)+\bar{D}_{n2}\cos h\lambda\left(vt-\ell_0\right) \tag{65}$$

In order to determine $\bar{d}_1$ and $\bar{d}_2$ in Eq.(65), we use the initial conditions $q_{n2}(0)=0$ and $\dot{q}_{n2}(0)=0$. After some operations, one readily finds

$$\bar{d}_1=-\frac{\Omega_n}{\omega_n}\left(\bar{A}_{n2}+\bar{C}_{n2}\right),\qquad \bar{d}_2=-\bar{B}_{n2}-\bar{D}_{n2} \tag{66}$$

The last form of $q_{n2}(t)$ in the first region can thus be written as

$$q_{n2}(t)\Big|_{t>\frac{L_0}{V\sqrt{L}}} = -\frac{\Omega_n}{\omega_n}\left(\bar{A}_{n2}+\bar{C}_{n2}\right)\sin\omega_n t-\left(\bar{B}_{n2}+\bar{D}_{n2}\right)\cos\omega_n t + \bar{A}_{n2}\sin\Omega_n t+\bar{B}_{n2}\cos\Omega_n t+\bar{C}_{n2}\sinh\Omega_n t+\bar{D}_{n2}\cosh\Omega_n t \tag{67}$$

Now, we insert Eq.(61) into Eq.(51) for the first part $t\le\dfrac{L_0}{V\sqrt{L}}$:

$$\ddot{q}_{n1}+\omega_n^2 q_{n1}=Q_{n1}(t)$$
$$=\frac{Mg}{\rho AL}f_{n1}(vt)-\frac{M}{\rho AL}f_{n1}(vt)\left[\sum_{m=1}^{N}\ddot{q}_m f_{m1}\right]-\frac{Mv^2}{\rho AL}f_{n1}(vt)\left[\sum_{m=1}^{N}q_m f''_{m1}\right]-\frac{2Mv}{\rho AL}f_{n1}(vt)\left[\sum_{m=1}^{N}\dot{q}_m f'_{m1}\right] \quad (68)$$

For the second part $t>\frac{L_0}{V\sqrt{L}}$, we have

$$\ddot{q}_{n2}+\omega_n^2 q_{n2}=Q_{n2}(t)$$
$$=\frac{Mg}{\rho AL}f_{n2}(vt)-\frac{M}{\rho AL}f_{n2}(vt)\left[\sum_{m=1}^{N}\ddot{q}_m f_{m2}\right]-\frac{Mv^2}{\rho AL}f_{n2}(vt)\left[\sum_{m=1}^{N}q_m f''_{m2}\right]-\frac{2Mv}{\rho AL}f_{n2}(vt)\left[\sum_{m=1}^{N}\dot{q}_m f'_{m2}\right] \quad (69)$$

Here, $q_{m1},\dot{q}_{m1},\ddot{q}_{m1},q_{m2},\dot{q}_{m2},\ddot{q}_{m2}$ are to be found from Eqs.(61) and (67). Writing Eq.(66) in Eq.(67) together, we have

$$\ddot{q}_n+\omega_n^2 q_n=\begin{cases}Q_{n1}, & t\le\frac{L_0}{V\sqrt{L}}\\ Q_{n2}, & t>\frac{L_0}{V\sqrt{L}}\end{cases} \quad (70)$$

Under zero initial conditions, the solution of Eq.(70) has the form

$$q_n(t)=\frac{1}{\omega_n}\int_0^t Q_n(\tau)\sin\omega_n(t-\tau)\,d\tau \quad (71)$$

or

$$q_n(t)=\frac{1}{\omega_n}\int_0^t Q_{n1}(\tau)\sin\omega_n(t-\tau)\,d\tau,\qquad t\le\frac{L_0}{V\sqrt{L}} \quad (72)$$

and

$$q_n(t)=\frac{1}{\omega_n}\int_0^{\frac{L_0}{V\sqrt{L}}} Q_{n1}(\tau)\sin\omega_n(t-\tau)\,d\tau+\frac{1}{\omega_n}\int_{\frac{L_0}{V\sqrt{L}}}^{t} Q_{n2}(\tau)\sin\omega_n(t-\tau)\,d\tau,$$
$$t>\frac{L_0}{V\sqrt{L}} \quad (73)$$

A very important point here is that if the time at which we wish to plot the curve is smaller than the time required for the load to arrive at the crack, one still must use $q_{n1}(t)$ obtained for $\phi_{n1}(a)$. When the load passes over the crack, then $\phi_{n2}(a)$ must be used on the right hand side of Eq.(51).

RESULTS AND DISCUSSION

Using the results of the present paper, the dimensionless deflection *y* versus modified time *t* has been plotted for various values of the variables. As an example, we assume

L = 20 m, EI = 2.7265.10^7 Nm^2, $\rho = 7800\ \mathrm{kg/m^3}$, $A = 0.2 \times 0.2$ m^2. The number of terms in the series has been taken as n = 4. It has been observed that the series rapidly converges. Since the right hand side of the differential equation is nonlinear and involves the unknown functions, as the number of terms in the series is increased, the solution time highly increases. Fig.(2) shows the deflection of the mid-point (X = 10 m) depicts the individual effects of centripetal and Coriolis forces for the crack location L_0 = 5 m: V = 20 m/s, $\gamma = 0.3$ and M = 5000 kg. It is obviously observed that the effect of centripetal force is greater than that of Coriolis force. The comparison of deflection y at the mid-point (X = 10 m) for various values of crack position L_0 = (1, 3, 5, 8, 10) for the values γ = 0.3, V = 20 m/s, M = 3000 kg is shown in Fig.(3). In order to determine the critical crack position, L_0 was taken (1,3,5,8,10) m. Since the moments are zero at the boundaries and almost zero at the mid point, we can expect that the critical crack position would be between these two values. Indeed, for the crack position X = 3 m, deflection becomes maximum. Such a critical point is also available on the second part of the beam where 10<X<20. Depending upon the values of the variables in the problem, these critical points must be determined for each time. .Figs. (4a), (4b) and (4c) depict the effects of the crack depth-ratio at the point X = 5 m, X = 10 m and X = 15 m, respectively. It is obviously seen that the dimensionless deflections increase with increasing values of γ. We see from these figures that the deflection is not strongly effected by the crack depth-ratio. In Figs. (5a), (5b) and (5c), taking L_0 = 8, V =20 m/s, M = 3000 kg , the variation of dimensionless deflection with dimensionless x is plotted for various instants of modified time t. The crack depth-ratio were taken γ = 0.1, γ = 0.3, γ = 0.6 in Figs. (5a), (5b) and (5c), respectively. The amplitude y slowly increases for increasing value of γ.

One of the main purpose of the present work is to see the effects of centripetal and Coriolis forces. In Fig.(6a), the effects of the constant force corresponding to $F = Mg$, the mass load involving inertia force ($Mg+Ma$) and the mass load with inertia force plus centripetal and Coriolis forces have been plotted for the values $\gamma = 0.1$, V = 20 m/s, L_0 = 8 m, M = 3000 kg. Solid line corresponds to constant force F. Dashed line corresponds to the mass load with inertia effect while dotted line corresponds to the mass load involving the totality of the effects. It is obvious that the deflections for the mass load are greater than that corresponding to the constant force F while the deflections for the mass load with inertia force plus centripetal and Coriolis forces are greater than that corresponding to mass load. As seen in Fig.(6b) and (6c), as γ increases, deflections also increase. Of course, these results are expected. Numerical calculations during this study have revealed that the centripetal forces are more effective on the vibration than Coriolis forces.

It should be expected that as the mass increases the centripetal and Coriolis forces would become more influential. Indeed, As depicted in Figs.(7a), (7b) and (7c) compared to the response under a constant force $F = Mg$, beam's behavior under mass loads with or without involving centripetal and Coriolis effects becomes quite different. It is clearly seen that the dynamic deflections increase with increasing values of the mass.

While formulating the present study, we have also corrected many problems in the literature. For example, we have pointed out that the eigen-functions are in general not orthonormal. We have proposed a normalization procedure to normalize them. The

present problem has been fully described and solved by giving all the details. Since some of the details was not given in some of the previous papers, it has been detected that the solution strategy has deficiency in many ways. It has been pointed out that the coefficients of the eigen-functions cannot be found explicitly, but they must be stated in terms of *A*'s , as in Eqs.(42). The coefficients *A*'s are obtained by means of fact that eigen-functions must also become orthonormal.

As an extension of the present study, the effect of a vehicle suspension system on the forced vibration of a bridge with a single and double-sided crack can be studied by involving the centripetal and Coriolis forces into the analysis.

CONCLUSION

Forced vibration of a cracked beam under moving mass loads is investigated in the present paper. Euler-Bernoulli beam theory has been used. Centripetal and Coriolis forces which become important in the case of long beams and mass load with high velocity have been inserted into the theory. The insertion of these terms into the theory makes the differential equation non-linear. Non-linear equation has been solved by iterative approach. The response of the system has been obtained in the form of Duhamel integral.

In the present work, some erroneous results given in some previous papers have been corrected and reformulated. For example, eigen-functions are orthogonal, but not orthonormal in general. But, they have been assumed to be orthonormal, a result which is wrong. The present study involves the correct solution of this problem and adds novelty.

In order to see the effects of centripetal force, Coriolis force and the crack, the results have been exemplified for various values of the parameters. It has been concluded that the response in the case of mass load appreciably differs from that of constant force *F*. Although regular curves for the response of the beam are obtained in the case of constant force, rather wavy curves are obtained in the case of mass loads due to the interaction between mass load and the beam. In addition, it has been observed that the response of the system is appreciably affected by the centripetal and Coriolis forces. Another important conclusion from the analysis is that the effect of centripetal force is greater than of the Coriolis force.

REFEERENCES

[1] Anifantis, N. and Dimarogonas, AD., "Post buckling behavior of transverse cracked columns", Computers and Structures, 18, p.351-356, (1984).

[2] Chondros, TG. and Dimarogonas AD., "Identification of cracks in welded joints of complex structures", Journal of Sound and Vibration, 69(4), p.531-538, (1980).

[3] Dimarogonas, AD., "Vibration of Cracked Structures: a state of the art review", Engineering Fracture Mechanics, 55(5), p.831-837, (1996).

[4] Haisty, BS. and Springer, WT., "A general beam element for use in damage assessment of complex structures", Journal of Vibration, Acoustic, Stress and Reliability in Design, 110, p.389-394, (1998).

[5] Shifrin, EI. and Ruotolo, R. “Natural frequencies of a beam with an arbitrary number of cracks”, Journal of Sound and Vibration, 222-3, p.409-423, (1999).
[6] Lin, HP., Chang, SC. and Wu, JD., “Beam vibrations with an arbitrary number of cracks”, Journal of Sound and Vibrations, 258(5), p.987-999, (2002).
[7] Chondros, TG., Dimarogonas, AD. and Yao, J., “A Continuous Cracked Beam Vibration Theory”, Journal of Sound And Vibration 215(1), p.17-34, (1998).
[8] Ostachowitz, WM. and Krawczuk, M., “Analysis of the effect of the cracks on the natural frequencies of a cantilever beam”, Journal of Sound And Vibration, 150, p.191-201, (1991).
[9] Rizos, PF. and Aspragathos, N., “Identification of crack location and magnitude in a cantilever beam from the vibration modes”, Journal of Sound And Vibration, 138, p.391-388, (1990).
[10] Liang, RY., Choy, FK. and Hu, I., “Detection of cracks in beam structures using measurements of natural frequencies”, Journal of Franklin Institute, 328(4), p.381-388, (1990).
[11] Lin, HP., “Direct and inverse methods on free vibration analysis of simply supported beams with a crack”, Engineering Structures, 26, p.427-436, (2004).
[12] Parhi, DR. and Behera, AK., “Dynamic deflection of a cracked shaft subjected to moving mass”, Transactions of the CSME , 21, p.295-316, (1997).
[13] Mahmoud, MA. “Stress intensity factors for single and double edge cracks in a simple beam subject to a moving load”, International Journal of Fracture, (11), p.151-161, (2001).
[14] Mahmoud, MA. and Abou Zaid, MA., “Dynamic Response of A Beam With A Crack Subject To A Moving Mass”, Journal of Sound and Vibration 256(4), p.591-603, (2002).
[15] Lin, HP. and Chang, SC., “Forced Responses Of Cracked Cantilever Beams Subjected To A Concentrated Moving Load”, International Journal of Mechanical Sciences, 48, p.1456–1463, (2006).
[16] Michaltsos, GT. and Kounadis, AN., “The effect of centripetal and Coriolis forces on the dynamic response of light bridges under moving loads”, Journal of Vibration and Control, 7, p.315-326, (2001).
[17] Kounadis, A., “A very efficient approximate method for solving non-linear boundary value problems”, Scientific papers of NTUA, 9(3,4), p.708-715, (1985).

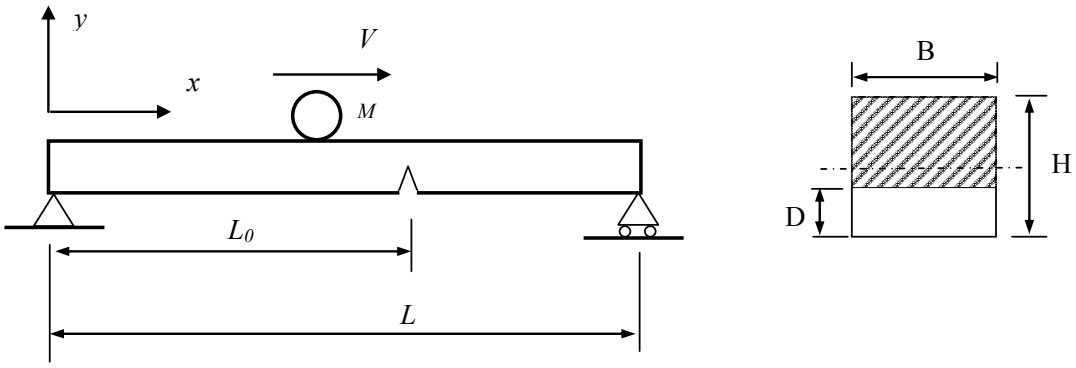

Fig.1. Simply supported cracked under a moving mass *M* with a constant velocity *V*.

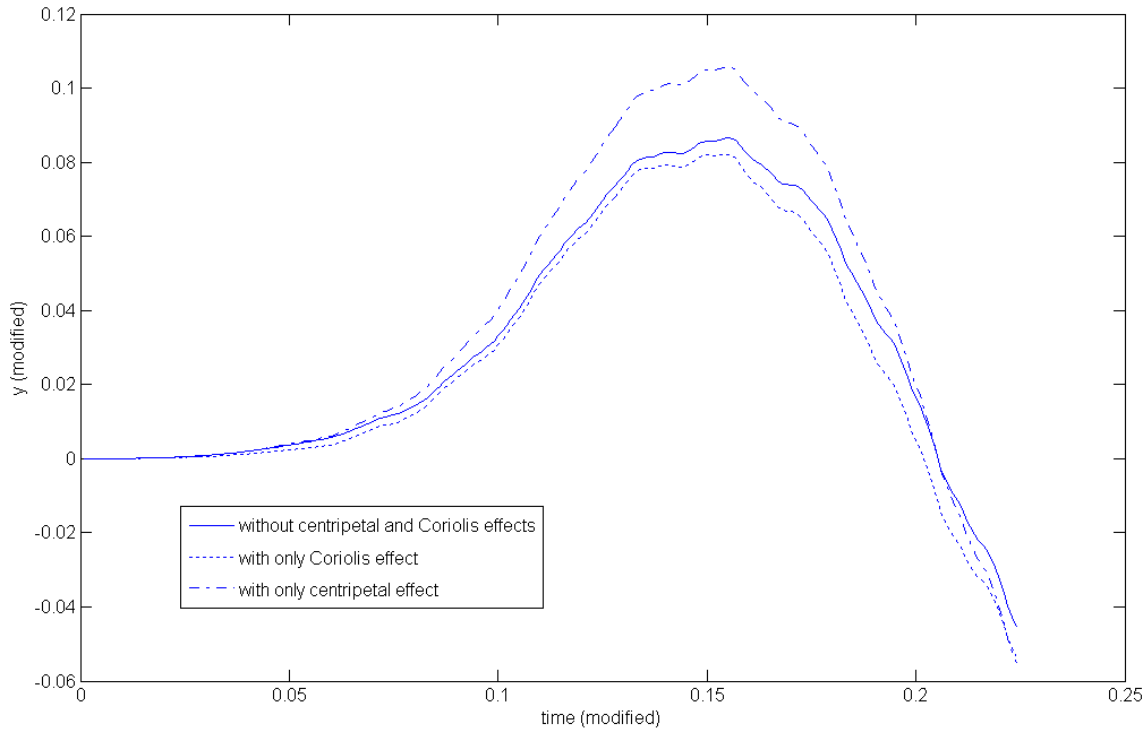

Fig 2. Comparison of centripetal and Coriolis effects:
X= 10 m, L_0 = 5 m, V = 20 m/s, M = 5000 kg, γ = 0,3.

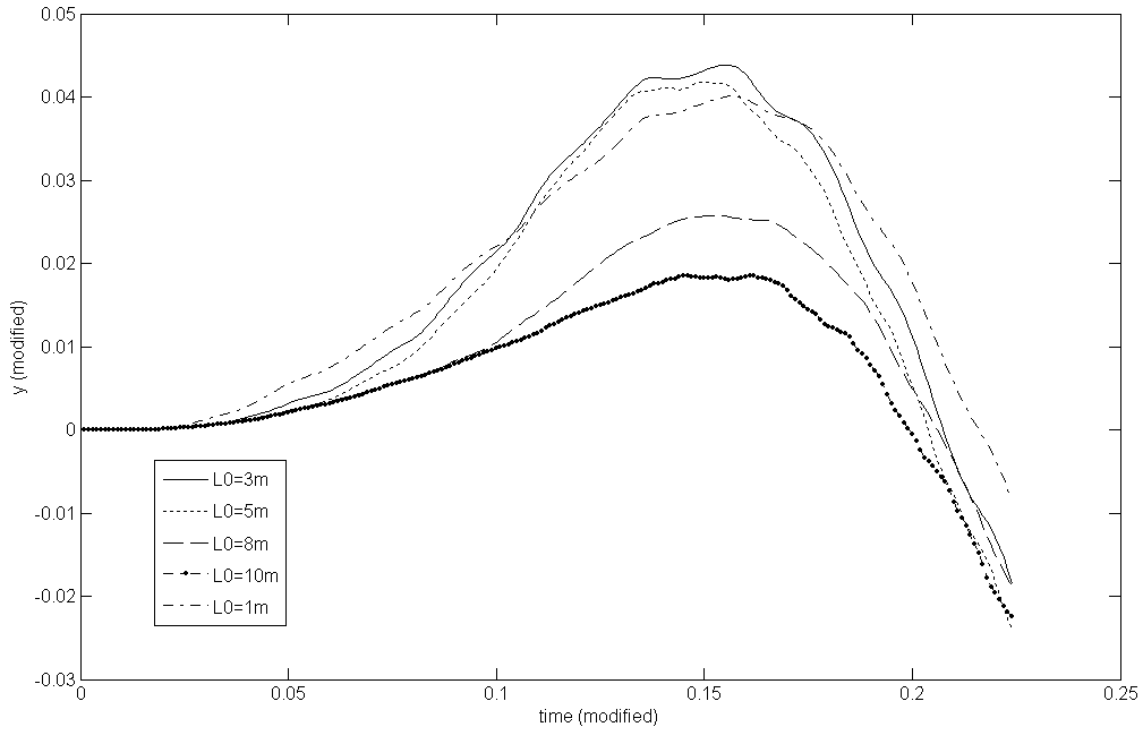

Fig 3. The effect of crack position on the response of the beam:
L_0 = (1, 3, 5, 8, 10) m γ = 0.3 m, V = 20 m/s, M = 3000 kg, X = 10 m.

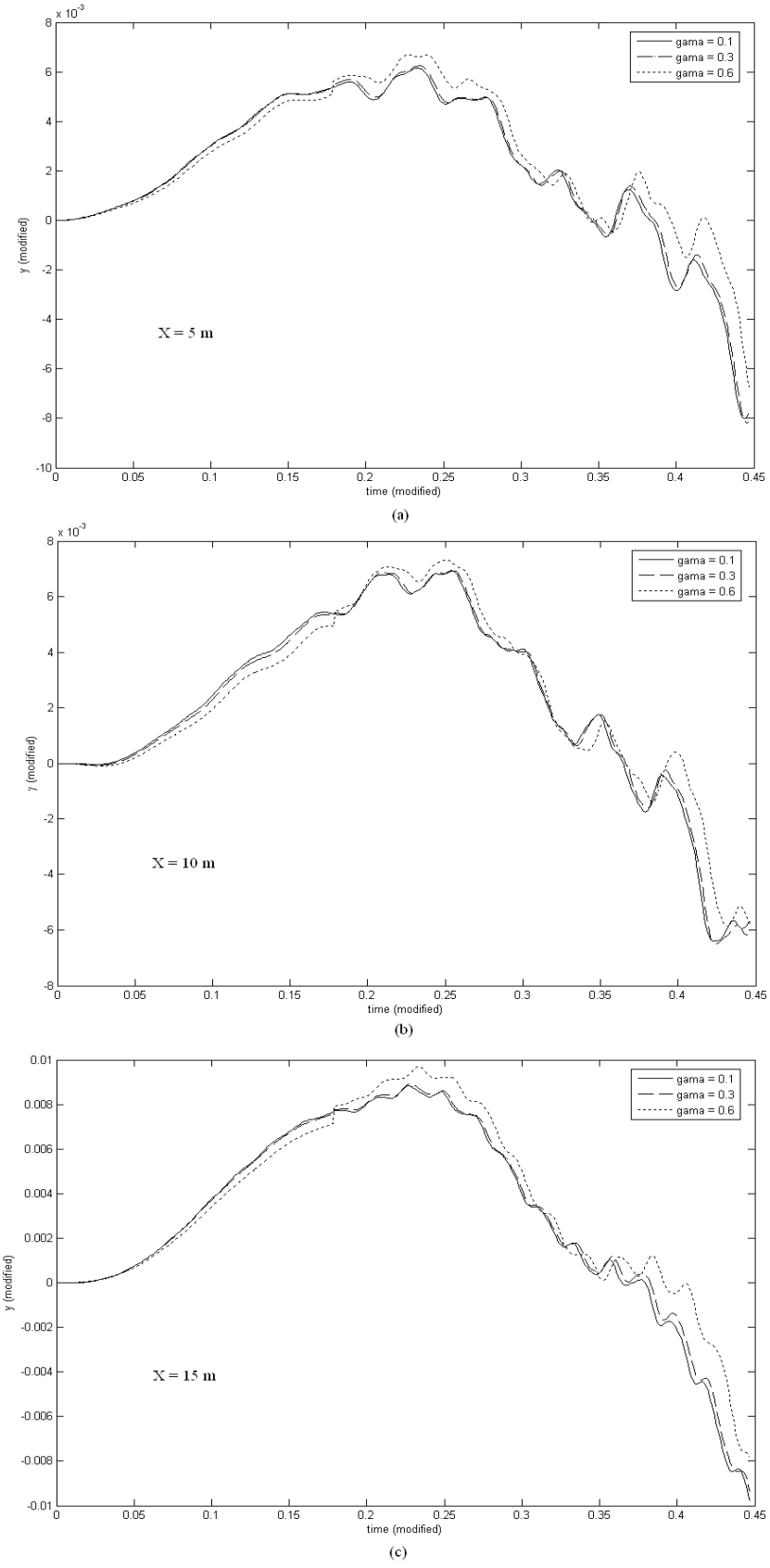

Fig 4. The effect of crack depth on the beam response at the point a.) X = 5 m, b.) X = 10 m, c.) X = 15 m : (γ = 0.1, 0.3, 0.6, L_0 = 8m, V = 10 m/s, M = 2000 kg)

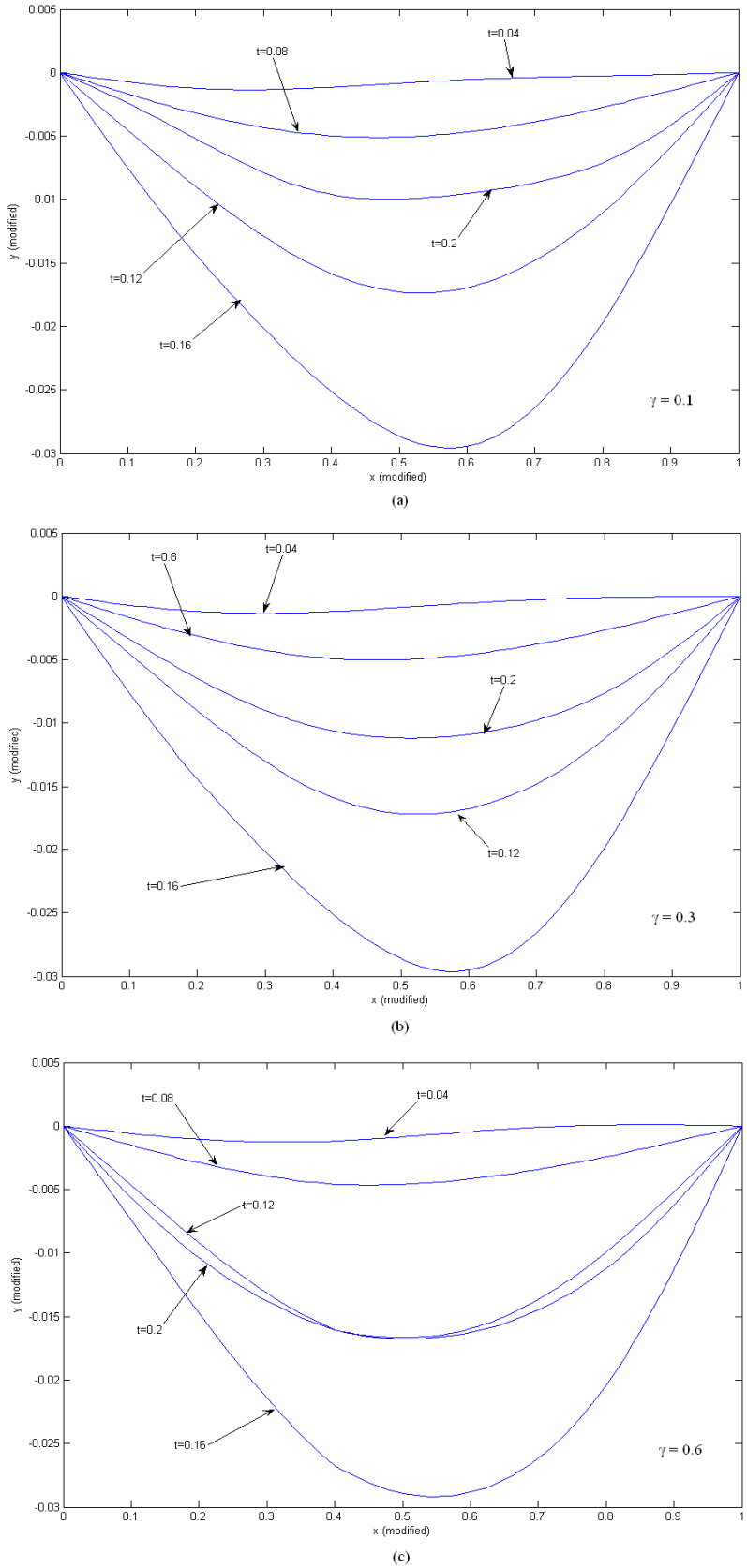

Fig 5. The shape of the beam during the passage of the moving load for: L_0=8, V=20 m/s, M=3000 kg, (t = 0.04, 0.0 8, 0.12, 0.16, 0.2). a) γ=0.1 b) γ=0.3 c) γ=0.6

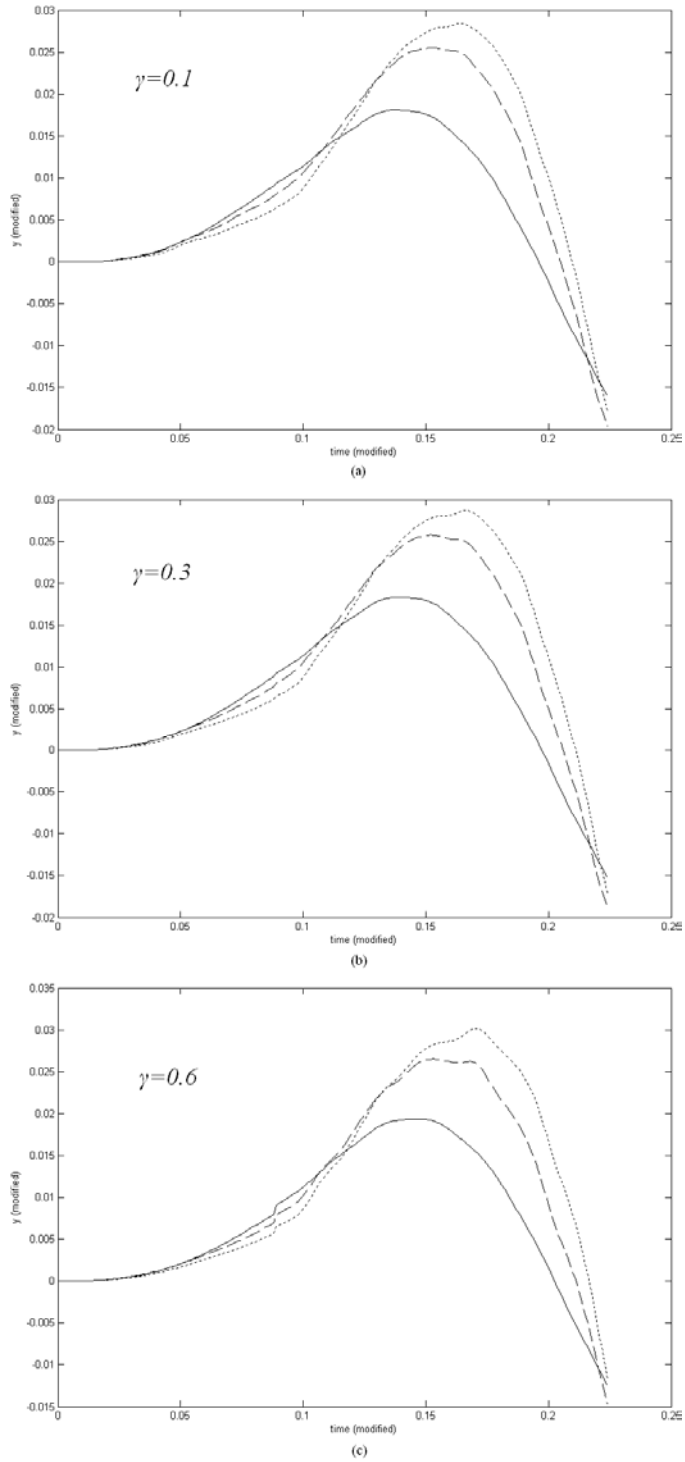

Fig 6. Comparison of the effects of constant force *F*, the mass load and the mass load involving centripetal and Coriolis forces: V = 20m/s, L_0 = 8m, M = 3000kg. Solid line corresponds to the constant force ($F = Mg$). Dashed line corresponds to the mass load without centripetal and Coriolis. Dotted line corresponds to the mass load with centripetal and Coriolis.

a.) γ = 0.1, b.) γ = 0.3, c.) γ = 0.6

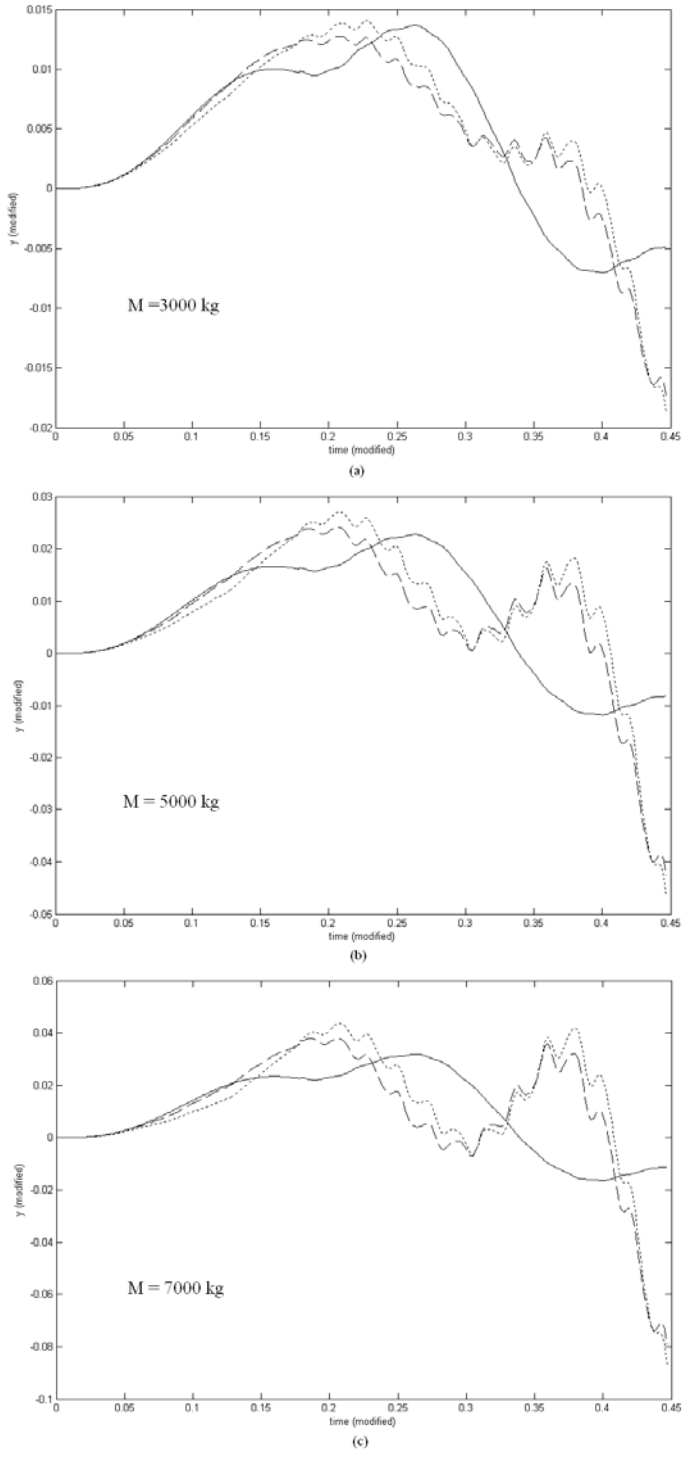

Fig 7. Comparison of the effects of constant force F , the mass load and the mass load involving centripetal and Coriolis forces : V = 10 m/s, L_0 = 8 m, γ = 0.3. Solid line corresponds to the constant force (F=Mg). Dashed line corresponds to the mass load without centripetal and Coriolis. Dotted line corresponds to the mass load with centripetal and Coriolis.

a.) M = 3000 kg, b.) M = 5000 kg, c.) M = 7000 kg